Appl Nanosci (2013) 3:189–195
DOI 10.1007/s13204-012-0123-7

ORIGINAL ARTICLE

Wet chemical synthesis and characterization of SnS_2 nanoparticles

Sunil H. Chaki · M. P. Deshpande · Devangini P. Trivedi · Jiten P. Tailor · Mahesh D. Chaudhary · Kanchan Mahato

Received: 29 October 2011 / Accepted: 9 April 2012 / Published online: 27 April 2012

Abstract The SnS_2 nanoparticles were synthesized at room temperature by simple wet chemical method. Stannic chloride pentahydrate ($SnCl_4{\cdot}5H_2O$) and thioacetamide (C_2H_5NS) were used as a source of Sn^{+4} ions and S^{-2} ions, respectively. The elemental composition of the as-synthesized SnS_2 nanoparticles was determined by energy dispersive analysis of X-ray. The structure and lattice parameters were determined by X-ray diffraction. The crystallite size was determined from XRD pattern using Scherrer's formula and Hall–Williamson plot. The transmission electron microscopy was employed to characterize the nanoparticles. The selected area electron diffraction pattern established the polycrystalline nature of SnS_2 nanoparticles. Surface topography of nanoparticles was studied employing scanning electron microscopy (SEM). The bandgap determined from the UV–Vis–NIR spectrum of as-synthesized SnS_2 nanoparticles showed blue shift in comparison with the bandgap of bulk SnS_2. The photoluminescence spectra at five different excitation wavelengths 250, 300, 350, 400 and 450 nm showed two strong emission peaks at wavelengths 550 and 825 nm. The obtained results are discussed in details.

Keywords SnS_2 nanoparticles · Wet chemical method · Transmission electron microscopy · Scanning electron microscopy · Optical absorbance · Photoluminescence

S. H. Chaki (✉) · M. P. Deshpande · D. P. Trivedi · J. P. Tailor · M. D. Chaudhary · K. Mahato
Department of Physics, Sardar Patel University, Vallabh Vidyanagar, 388 120 Gujarat, India
e-mail: sunilchaki@yahoo.co.in

Introduction

In the recent years, zero-dimensional nanostructural metal sulphide semiconductors have attracted much attention due to their physical and chemical properties. The metal sulphide semiconductors of zero-dimension are currently recognized as advanced inorganic materials with nonconventional applications due to the quantum size effect. These nanostructures in particular show remarkable electronic (Yi and Schwarzacher 1999), magnetic (Ross et al. 2002), optical (Zhang et al. 2011), etc. properties, which have great potential applications in the next generation of nanodevices (Zach et al. 2000). Among the semiconductors, tin disulfide (SnS_2) is an important CdI_2-type IV–VI group layered semiconductor with an optical band gap of about 2.2–2.35 eV (Zhang et al. 2010; Yang et al. 2009) which is little smaller than that of CdS. Such a tuneable band gap of SnS_2 makes it a potential candidate for efficient solar cell (Loferski 1956). It is also of interest in holographic recording system and electrical switching (Chun et al. 1994; Patil and Fredgold 1971). SnS_2 is non-poisonous, relatively inexpensive and chemically stable in acid or neutral aqueous solution, thus it has the potential to be a good visible light-sensitive photocatalyst (Zhang et al. 2010; Yang et al. 2009; He et al. 2007). It is also an interesting material that belongs to the class of isomorphic materials that exhibit a strong anisotropy of optical properties (Agrawal et al. 1994).

Many synthesis methods have been employed to prepare SnS_2 nanoparticles including soft chemical reaction, solid-state reaction, sol–gel process, hydrothermal (Li et al. 2009; Rao et al. 2004) microwave heating (Lokhande 1990) photo etching (Gaponendo 1998), and reverse micelles, etc. The wet chemical method is relatively inexpensive, non-toxic, less time consuming and very simple because it contains

few chemicals and does not required any sophisticated expensive instruments. In this paper, the authors report the synthesis of SnS_2 nanoparticles by a wet chemical method at room temperature (R.T.) using stannic chloride pentahydrate ($SnCl_4{\cdot}5H_2O$) and thioacetamide (C_2H_5NS) as a precursor. The study of the stoichiometric composition, structural, surface morphology, optical and luminescence properties of the as-synthesised nanoparticles was carried out.

Experimental

Synthesis of SnS_2 nanoparticles

All chemicals for the synthesis of SnS_2 nanoparticles such as stannic chloride pentahydrate ($SnCl_4{\cdot}5H_2O$), thioacetamide (C_2H_5NS), and concentrated hydrochloric acid (HCl 35 % pure A.R.) were of analytical grade and used as received without further purification. In the typical synthesis, 0.806 g (2.3 mmol) of $SnCl_4{\cdot}5H_2O$ was dissolved in 2 ml of concentrated HCl acid (35 %, w/w) in a 100 ml beaker. Then, 30 ml distilled water was added and stirring was done for 5 min. It acts as a source of Sn^{+4} ions. After 5 min stirring, 0.25 g (3.3 mmol) of thioacetamide was added to the solution under constant stirring. Thioacetamide was the source of S^{-2} ions. The stirring was continued for 3 h. During this period, solution turned into yellow color and lastly 18 ml distilled water was added to make the final solution of 50 ml. The final solution was kept isolated for 25–30 min to allow particles to settle down at the bottom of the beaker. The yellow precipitates settled at the bottom of the beaker were filtered and washed with distilled water followed with methanol for several times to obtain SnS_2 nanoparticles. After multiple washes, they were dried in oven at 40 °C for 6 h. Figure 1 show the photograph of the synthesized SnS_2 nanoparticles yield obtained after wash.

Characterization of SnS_2 nanoparticles

The stoichiometric compositions of the as-synthesized SnS_2 nanoparticles were studied with the help of energy dispersive analysis of X-ray (EDAX) employing Philips ESEM having 10–20 keV energy range of the beam. The structural characterization of the particles was done by X-ray diffraction (XRD) using Philips X-ray Diffractometer Xpert MPD employing CuK_α radiation. The as-synthesized SnS_2 nanoparticles were further investigated by transmission electron microscopy (TEM) employing JEOL, JEM 2100. The surface topography study was done by LEO 1430 VP scanning electron microscopy (SEM). An optical absorption study was carried out using a UV–Vis-NRI spectrophotometer (Shimadzu UV-240). The Photoluminescence spectra of SnS_2 nanoparticles were studied using Horiba Yvon FluroMax-4 Spectrofluorometer.

Fig. 1 Photograph of the room temperature synthesized SnS_2 nanoparticles

Results and discussion

Synthesis reaction

In the synthesis of SnS_2 nanoparticles by wet chemical technique, stannic chloride pentahydrate ($SnCl_4{\cdot}5H_2O$) dissociate to form tin ions and thioacetamide (C_2H_5NS) is the source of sulfur ions. The concentration of tin and sulphide ions is maintained low to avoid immediate precipitation. The SnS_2 nanoparticles are formed by the precipitation reaction between Sn^{4+} and H_2S produced by the hydrolysis of thioacetamide. Here, thioacetamide reacts with water at the reaction condition to slowly produce H_2S. The H_2S (bubble) reacts with Sn^{4+} to homogeneously form SnS_2 nanoparticles. The formation of SnS_2 nanoparticles may be described by Eqs. (1) and (2) as follows:

$$CH_3-CS-NH_2 + 2H_2O \Rightarrow CH_3-CO_2-NH_4 + H_2S \quad (1)$$

$$2H_2S + Sn^{4+} \Rightarrow SnS_2 + 4H^+ \quad (2)$$

Stoichiometric composition studies

The stoichiometric compositions and purity of the synthesized SnS_2 nanoparticles were determined by energy dispersive analysis of X-rays (EDAX) techniques. Figure 2 shows the EDAX spectrum of room temperature synthesized SnS_2 nanoparticles. The obtained weight percentage from EDAX spectrum and the standard weight percentage of tin (Sn) and sulphur (S) elements are tabulated in

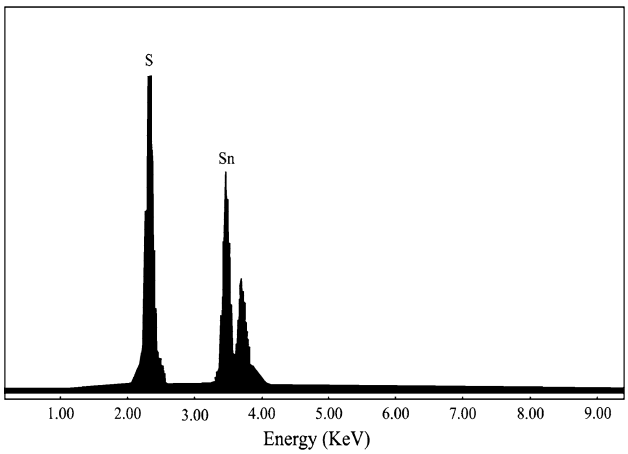

Fig. 2 EDAX spectra of as-synthesized SnS_2 nanoparticles (R.T.)

Table 1 for SnS_2 nanoparticles. The weight percentage data shows that the synthesized SnS_2 nanoparticles are slightly rich in tin content. The EDAX spectrum also showed that the synthesized SnS_2 nanoparticles are free of any other impurities and contaminants. The atomic percentage data of tin and sulphur are also tabulated in Table 1.

Structural studies

The structure, lattice parameters and phase purity of the synthesized SnS_2 nanoparticles were determined by X-ray diffraction (XRD). Figure 3 shows the XRD pattern, all the peaks in the XRD pattern can be readily indexed to the pure hexagonal phase of SnS_2 with lattice constants $a = 3.648$ Å and $c = 5.899$ Å, which are in good agreement with the standard JCPDS (File No. 23-0677) data.

Average crystallite size was estimated by Scherrer's formula (Panda et al. 2007),

$$L = \frac{K\lambda}{\beta_{2\theta}\cos\theta} \tag{3}$$

where k is the shape factor which typically has value of unity for the spherical shape particle; β is the broadening of diffraction line measured at half maximum intensity (radians), λ is the wavelength of CuK_α radiation and θ is the Bragg's angle. The crystallite sizes of SnS_2 nanoparticles were estimated to be around 3.60 nm from the Scherrer's formula.

The crystallite size and the micro strain in the as-synthesized SnS_2 nanoparticles were estimated by Hall–Williamson relation (Williamson and Hall 1953).

$$\frac{\beta\cos\theta}{\lambda} = \frac{1}{L} + \frac{\varepsilon 4\sin\theta}{\lambda}. \tag{4}$$

The Hall–Williamson equation includes the Scherrer's term of crystallite size (L) and the micro strain term (ε). Here β is full width at half maximum (FWHMs) of the diffraction peaks. The plot of $(\beta\cos\theta)/\lambda$ versus $4(\sin\theta)/\lambda$ for the as-synthesized nanoparticles is shown in the Fig. 4. The reciprocal of an intercept on $(\beta\cos\theta)/\lambda$ axis gives the average crystallite size L. The value of average crystallite size L thus obtained from the plot is $\sim$3.23 nm, which is in good agreement with the crystallite size determined by Scherrer's equation. The slope of the plot gives the amount of residual strain of (-0.0047). The negative value of residual strain for the SnS_2 nanoparticles indicates it to be compressive strain.

Table 1 Stoichiometric composition of SnS_2 nanoparticles (R.T.) determined by EDAX

Element	Weight percentage (%)		Atomic percentage (%)
	Observed value	Calculated value	
Sn (K)	68.42	64.93	36.96
S (K)	31.58	35.07	63.04

TEM and SAED studies

The morphology and structure of the as-synthesized SnS_2 nanoparticles were studied by transmission electron microscopy (TEM). Figure 5a, b shows a typical high-resolution transmission electron microscopy (HRTEM) image of SnS_2 nanoparticles. The image, Fig. 5a, shows nanoparticles to be spherical in shape, with each nanoparticle displaying lattice fringes, suggesting their crystalline nature. The average particle diameter determined from the TEM image comes out around 3.87 nm. This is in good agreement with the size determined from the XRD. The fringe has lattice spacing of about 0.312 nm, Fig. 5b, which corresponds to {100} crystal planes of hexagonal structured SnS_2 (JCPDS No. 23-0677) (Zhu et al. 2006). The corresponding selected area electron diffraction (SAED) pattern in Fig. 6 shows (002), (003) and (111) planes to be prominent, which is consistent with the XRD results presented above.

Surface topography study

The SEM study of the as-synthesized SnS_2 nanoparticles reveals the surface topography. The typical SEM image of the SnS_2 nanoparticles is shown in Fig. 7. The nanoparticles are spherical in shape, corroborating the observations of TEM. They are densely packed possessing compact texture with no pin holes or cracks.

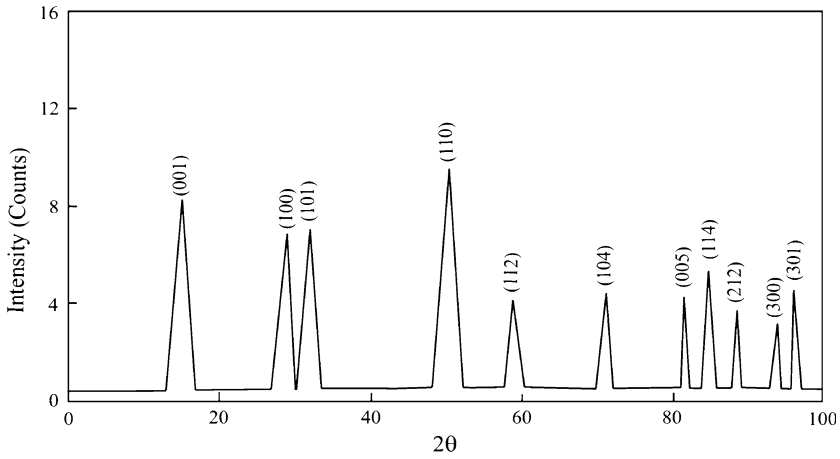

Fig. 3 X-ray diffractrogram of SnS_2 nanoparticles (R.T.)

Optical study

The absorption spectrum of SnS_2 nanoparticles was recorded by UV–Vis–NIR spectrophotometer. The SnS_2 nanoparticles were ultrasonically dispersed in acetone. Figure 8 shows the absorption spectrum of SnS_2 nanoparticles synthesized at room temperature and it can be seen that the absorption edge lies at 480 nm corresponding to energy value of 2.61 eV. The absorption edge observed at 480 nm clearly indicates a blue shift in comparison to the bulk SnS_2 having absorption edge nearly at 507 nm (Takagahara 1993; Hanumura 1988).

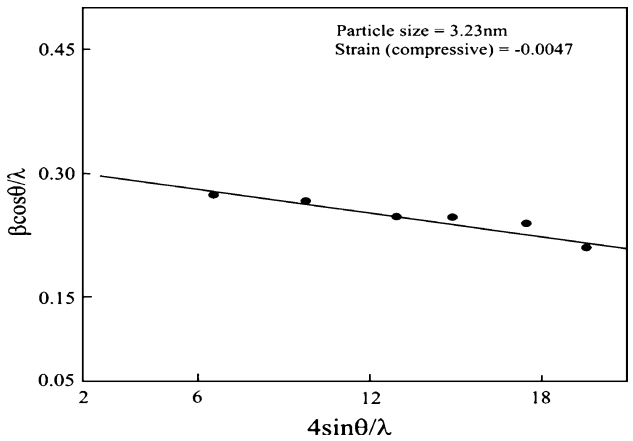

Fig. 4 Hall-Williamson plots for SnS_2 nanoparticles synthesised at room temperature

The optical energy bandgap of SnS_2 nanoparticles was determined from the absorption spectrum using the near-band edge absorption relation (Yue et al. 2009).

$$(\alpha hv)^n = A(hv - E_g)$$

where A is the optical transition dependent constant, E_g is the optical energy bandgap, v is the frequency of incident beam, h is the Planck's constant and n characterizes the transition. The absorption coefficient (α) was determined by the equation (Ingle and Crouch 1988),

$$\alpha = \frac{A\rho}{Mcl}\,(\mathrm{cm})^{-1}$$

where A is the absorbance of light through sample, ρ is the density of SnS_2, M is the molecular weight of SnS_2, c is the sample concentration dispersed in acetone and l is the path length of light.

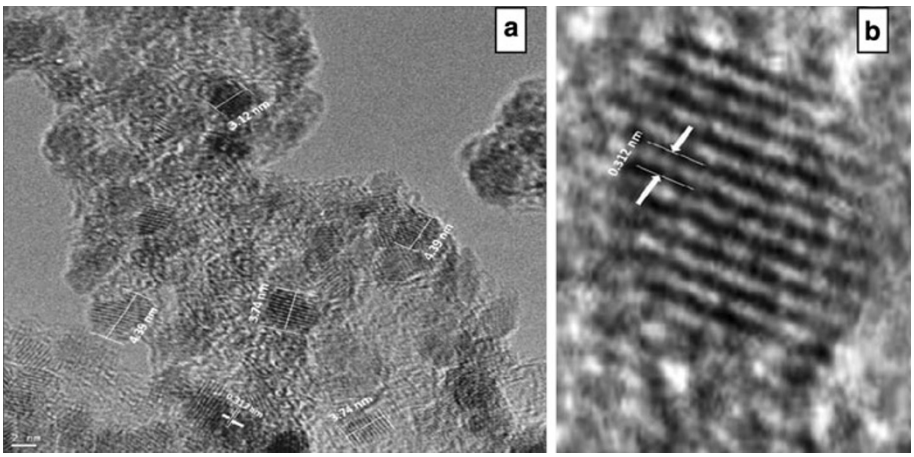

Fig. 5 HRTEM image of SnS_2 nanoparticles synthesised at room temperature

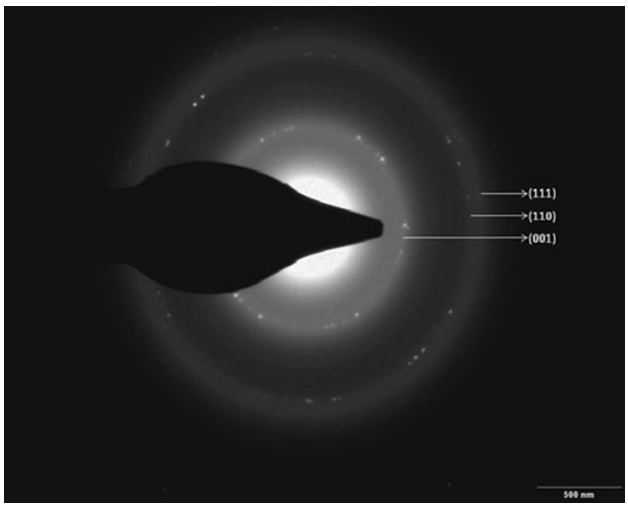

Fig. 6 Selected area electron diffraction pattern of SnS_2 nanoparticles synthesised at room temperature

The analysis of equation showed that, $n = 2$ fitted for the as-synthesized SnS_2 nanoparticles confirming direct allowed transition. The plot of $(\alpha hv)^2$ versus hv for SnS_2 nanoparticles is shown in Fig. 9. The intercept of the straight line on the photon energy axis gives the optical bandgap value E_g of 3.82 eV, which is higher than that of bulk SnS_2 optical bandgap, clearly showing the blue shift arising due to size effect.

Photoluminescence study

The photoluminescence spectra of the as-synthesized SnS_2 nanoparticles were recorded for five excitation viz 250, 300, 350, 400, and 450 nm wavelengths. The spectra obtained for SnS_2 nanoparticles are shown in the Fig. 10.

The spectra exhibit two strong emission peaks at around 550 and 825 nm. The emission at 550 nm (2.25 eV)

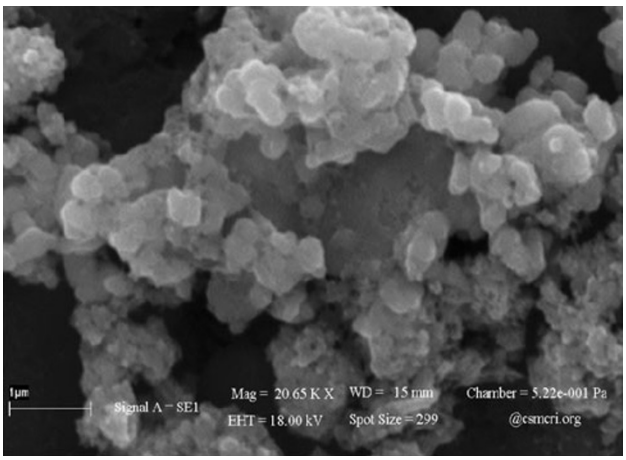

Fig. 7 SEM image of SnS_2 nanoparticles (R.T.)

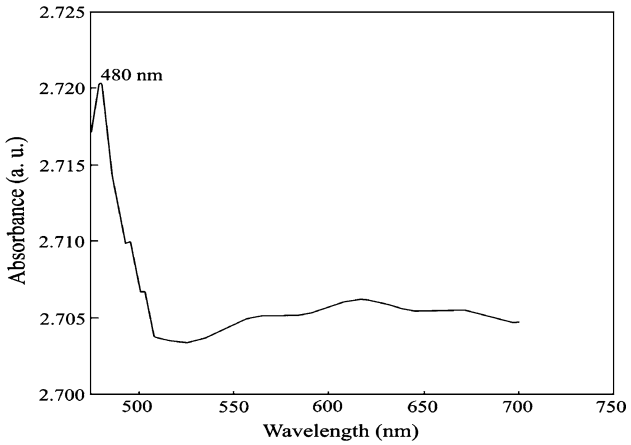

Fig. 8 Absorption spectrum of SnS_2 nanoparticles (R.T.)

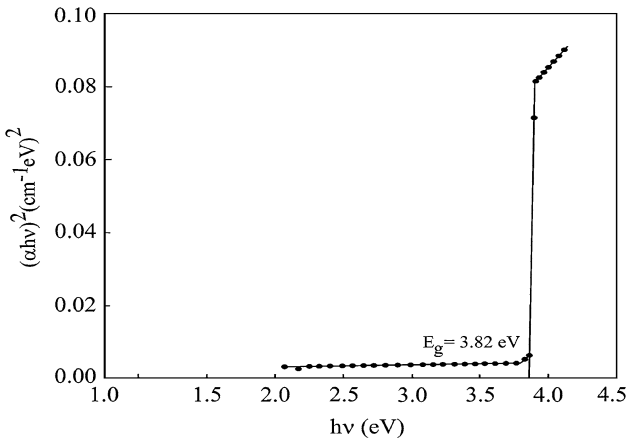

Fig. 9 Plot of $(\alpha hv)^2$ versus hv

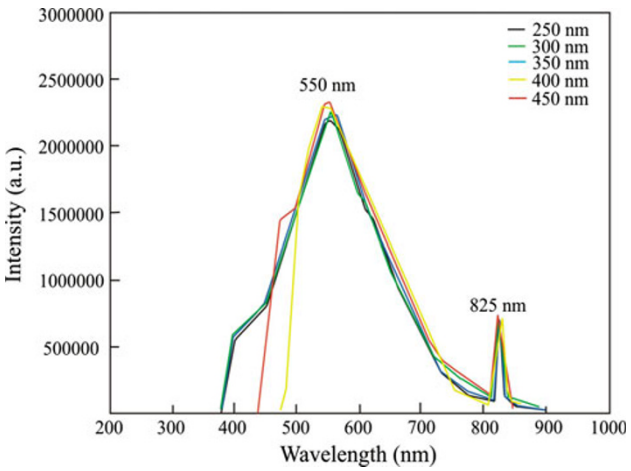

Fig. 10 PL emission spectra of the SnS_2 nanoparticles synthesized at room temperature

corresponds to radiative recombination of quantum confined electron–hole pair whose energy is smaller than the energy bandgap of nanoparticles. The radiative recombination of

excitons is by absorption of electrons lying at higher excited energy levels (Gaponendo 1998). The possible explanation for the origin of the latter peak at 825 nm wavelength might be from the inner deep level emission (Gajendiran and Rajendran 2011). This deep level arises due to the stoichiometric variation in SnS_2 nanoparticles. It was also observed from the PL spectra of the SnS_2 nanoparticles that for five excitation wavelengths, the emissions intensity remains same, meaning the emission intensity is independent of excitation wavelengths.

Conclusions

The SnS_2 nanoparticles have been successfully synthesized by simple wet chemical technique at room temperature. The synthesis was carried out at ambient condition using AR grade non-toxic chemicals without requirement of any sophisticated instruments. The EDAX analysis confirms that the synthesized SnS_2 nanoparticles were perfectly stoichiometric and do not contain any other impurity in them. The X-ray diffraction showed that the synthesized SnS_2 nanoparticles had hexagonal structure. The determined lattice parameters were in good agreement with the reported data. The crystallite size determined from XRD, using Scherrer's equation (3.60 nm) and Hall–Williamson's plot (3.23 nm) were in good agreement with each other. The residual strain determined from Hall–Williamson's plot was (−0.0047), the negative value indicates it to be the compressive strain. The HRTEM image shows nanoparticles to be spherical in shape, with each nanoparticles displaying lattice fringes, suggesting their crystalline nature. The average particle diameter determined from the TEM image is around 3.87 nm, in good agreement with the size determined from the XRD. The HRTEM clearly shows fringes having lattice spacing of about 0.312 nm, which corresponds to {100} planes of hexagonal structured SnS_2. The SEM image show nanoparticles are spherical in shape corroborating TEM observation. They are densely packed possessing compact texture with no pin holes or cracks. The optical bandgap energy 3.82 eV was calculated from the optical absorbance spectrum of the as-synthesized SnS_2 nanoparticles, which is higher than that of bulk SnS_2 optical bandgap, which clearly shows the blue shift arising due to size effect. The photoluminescence spectra of the SnS_2 nanoparticles for five excitation viz 250, 300, 350, 400, and 450 nm wavelengths exhibit two strong emission peaks at around 550 and 825 nm. The PL spectra also showed that for five excitation wavelengths, the emissions intensity remains same which means the emission intensity is independent of excitation wavelengths.

Acknowledgments The authors are thankful to the Sophisticated Instrumentation Centre for Applied Research & Testing (SICART), Vallabh Vidyanagar, Gujarat, India for EDAX, XRD and UV–Vis–NIR spectrophotometer analysis. The authors are grateful to the Central Salt and Marine Chemicals Research Institute (CSMCRI), Bhavnagar, Gujarat, India for HRTEM and SEM analysis. The authors are thankful to the Faculty of Engineering and Technology, M. S. University of Baroda, Vadodara, Gujarat, India for photoluminescence analysis on our samples.

References

Agrawal A, Patel PD, Lakshminarayana D (1994) Single crystal growth of layered tin monoselenide semiconductor using a direct vapour transport technique. J. Crystal Growth 142:344. doi:10.1016/0022-0248(94)90343-3

Chun D, Walser RM, Bene RW, Courtney TH (1994) Polarity-dependent memory switching in devices with SnSe and $SnSe_2$ crystals. Appl Phys Lett 24:344. doi:10.1063/1.1655019

Gajendiran J, Rajendran V (2011) Synthesis of SnS_2 nanoparticles by a surfactant-mediated hydrothermal method and their characterization. Adv Nat Sci Nanosci 2:015001–015004. doi:10.1088/2043-6262/2/1/015001

Gaponendo SV (1998) Optical properties of semiconductors nanocrystals. Cambridge University Press, Cambridge. doi:10.2277/0521582415

Hanumura E (1988) Very large optical nonlinearity of semiconductor microcrystallites. Phys Rev B 37:1273–1279. doi:10.1103/PhysRevB.37.1273

He HY, Huang JF, Cao LY, Wu JP, He Z, Luo L (2007) Photocatalytic activity of mixture of SnS_2 and TiO_2 powders in destruction of methyl orange in water. J Optoelectron Adv Mater 9:3781–3784

Ingle JDJ, Crouch SR (1988) Spectrochemical analysis. Prentice Hall, Englewood Cliffs, pp 372–381

Li Y, Xie H, Tu J (2009) Nanostructured SnS/carbon composite for supercapacitor. Mater Lett 63:1785–1787. doi:10.1016/j.matlet.2009.05.036

Loferski JJ (1956) Theoretical considerations governing the choice of the optimum semiconductor for photovoltaic solar energy conversion. J Appl Phys 27:777. doi:10.1063/1.1722483

Lokhande CD (1990) A chemical method for tin disulphide thin film deposition. J Phys D Appl Phys 23:1703. doi:10.1088/0022-3727/23/12/032

Panda SK, Antonakos A, Liarokapis E, Bhattacharya S, Chaudhuri S (2007) Optical properties of nanocrystalline SnS_2 thin films. Mater Res Bull 42:576–583. doi:10.1016/j.materresbull.2006.06.028

Patil SG, Fredgold RH (1971) Electrical and photoconductive properties of SnS_2 crystals. J Pure Appl Phys 4:718. doi:10.1088/0022-3727/4/5/312

Rao MM, Jayalakshmi M, Reddy RS (2004) Time-selective hydrothermal synthesis of SnS nanorods and nanoparticles by thiourea hydrolysis. Chem Lett 33:1044. doi:10.1246/cl.2004.1044

Ross CA, Hwang M, Shima H, Smith HI, Farhoud M, Savas TA (2002) Magnetic properties of arrays of electrodeposited nanowires. J Magn Magn Mater 249:200–207. doi:10.1016/S0304-8853(02)00531-0

Takagahara T (1993) Effects of dielectric confinement and electron-hole exchange interaction on excitonic states in semiconductor quantum dots. Phys Rev B 47:4569–4584. doi:10.1103/PhysRevB.47.4569

Williamson GK, Hall WH (1953) X-ray line broadening from filed aluminium and wolfram. Acta Metall 1:22–31. doi:10.1016/0001-6160(53)90006-6

Yang C, Wang W, Shan Z, Huang F (2009) Preparation and photocatalytic activity of high-efficiency visible-light-responsive photocatalyst SnS_x/TiO_2. J Solid State Chem 182:807–812. doi:10.1016/j.jssc.2008.12.018

Yi G, Schwarzacher W (1999) Single crystal superconductor nanowires by electrodeposition. Appl Phys Lett 74:1746. doi:10.1063/1.123675

Yue GH, Peng DL, Yan PX, Wang LS, Wang W, Luo XH (2009) Structure and optical properties of SnS thin film prepared by pulse electrodeposition. J Alloy Compd 468:254–257. doi:10.1016/j.jallcom.2008.01.047

Zach MP, Ng KH, Penner RM (2000) Molybdenum nanowires by electrodeposition. Science 290:2120. doi:10.1126/science.290.5499.2120

Zhang YC, Du ZN, Li SY, Zhang M (2010) Novel synthesis and high visible light photocatalytic activity of SnS_2 nanoflakes from $SnCl_2{\cdot}2H_2O$ and S powders. Appl Catal B 95:153–159. doi:10.1016/j.apcatb.2009.12.022

Zhang YC, Du ZN, Li KW, Zhang M, Dionysiou DD (2011) High-performance visible-light-driven SnS_2/SnO_2 nanocomposite photocatalyst prepared via in situ hydrothermal oxidation of SnS_2 nanoparticles. Appl Mater Interface 3:1528–1537. doi:10.1021/am200102y

Zhu H, Ji X, Yang D (2006) Hydrothermal synthesis and characterization of novel aloe-like SnS_2 nanostructures. J Mater Sci 41:3489–3492. doi:10.1007/s10853-005-5911-y